

# Copper hexacyanoferrate multilayer films on glassy carbon electrode modified with 4-aminobenzoic acid in aqueous solution

Guocheng Yang<sup>a,b</sup>, Yan Shen<sup>a,b</sup>, Mingkui Wang<sup>a,b</sup>, Hongjun Chen<sup>a,b</sup>,  
Baifeng Liu<sup>a</sup>, Shaojun Dong<sup>a,b,\*</sup>

<sup>a</sup> State Key Laboratory of Electroanalytical Chemistry, Changchun Institute of Applied Chemistry,  
Chinese Academy of Sciences, Changchun, Jilin 130022, PR China

<sup>b</sup> Graduate School of the Chinese Academy of Sciences, Beijing 100039, PR China

Received 11 January 2005; received in revised form 25 May 2005; accepted 25 May 2005

Available online 27 June 2005

## Abstract

4-Aminobenzoic acid (4-ABA) was covalently grafted on a glassy carbon electrode (GCE) by amine cation radical formation during the electrooxidation process in 0.1 M KCl aqueous solution. X-ray photoelectron spectroscopy (XPS) measurement proves the presence of 4-carboxylphenylamine on the GCE. Electron transfer processes of  $\text{Fe}(\text{CN})_6^{3-}$  in solutions of various pHs at the modified electrode are studied by both cyclic voltammetry (CV) and electrochemical impedance spectroscopy (EIS). Changing the solution pH would result in the variation of the terminal group's charge state, based on which the surface  $\text{p}K_a$  values were estimated. The copper hexacyanoferrate (CuHCF) multilayer films were formed on 4-ABA/GCE prepared in aqueous solution, and which exhibit good electrochemical behavior with high stability. © 2005 Elsevier B.V. All rights reserved.

**Keywords:** 4-Aminobenzoic acid; Covalent modification; Glassy carbon electrode; Copper hexacyanoferrate; Self-assembly multilayer film

## 1. Introduction

Modification of highly ordered mono- and multilayer on carbon surfaces, which plays an important role in catalysis, analytical and biotechnological applications. Recently, free radical grafting methods, through electrochemical reduction and oxidation of diazonim salts and arylacetates, amino-containing compounds respectively at carbon electrodes forming covalent bond between carbon electrode surface and the modifier in nonaqueous solution [1–18], provide an efficient route for the modification of carbon surface with great significance. However, by using the methods mentioned above, the modification conditions in organic phase are especially rigorous. For example, the organic solvent and supporting electrolyte used should be treated free of water before modification; the saturated solution in reference electrode must be anhydrous, water should be refrained

from importing during the whole process, and test solution containing modifier must be stored carefully, etc. It can be seen that the modification process in organic phase is loaded with trivial detail. On the other hand, attention has been paid to seeking a more convenient modification condition at carbon surface such as in aqueous solution that can much simplify the operating processes. Covalent modification of *r*-aminobenzene sulfonic acid on GCE in aqueous solution was reported recently [19]. Electrochemical reduction of a mixture with 4-aminobenzo-15-crown-5 and  $\text{NaNO}_2$  in aqueous solution was also reported to generate diazotized benzo-15-crown-5 [20]. In this paper, we try to modify GCE with 4-aminobenzoic acid (4-ABA) via electrochemical oxidation in aqueous solution, and get process. The resulted film with 4-ABA modified on GCE from aqueous solution is quite stable and the fabrication process is very simple and versatile.

Prussian blue (PB) and its analogues are an interesting group of polymeric inorganic compounds for surface modification due to their attractive physicochemical characteristics such as electrochromism, ion exchange, and molecular mag-

\* Corresponding author. Tel.: +86 431 5262101; fax: +86 431 5689711.  
E-mail address: [dongsj@ns.ciac.jl.cn](mailto:dongsj@ns.ciac.jl.cn) (S. Dong).

netism besides electrocatalytic properties [21–29]. Generally, thin films of PB and its analogues were electrodeposited from a mixture of solution containing metal salt and the corresponding metalcyanide or by dissolution and precipitation method [22]. Herein, we propose a simple approach for construction of metal hexacyanoferrate (MHCF) mono- and multilayers, such as copper hexacyanoferrate (CuHCF), on the 4-ABA/GCE prepared in aqueous solution. The fabrication strategy of CuHCF multilayer on 4-ABA/GCE is based on complexation between metal ion and with hexacyanoferrate and covalent bonding on carbon surface. The resulting MHCF/4-ABA/GCE modified electrode has good electrochemical behavior with high stability.

## 2. Experimental section

### 2.1. Reagents

4-Aminobenzoic acid (4-ABA) was purchased from Aldrich. The solution of 4-ABA was freshly prepared for each modification. Other reagents were of analytical reagent grade and used as received. Buffer solution were prepared from 0.1 M NaAc + HAc (pH 3–6), 0.1 M Na<sub>2</sub>SO<sub>4</sub> + H<sub>2</sub>SO<sub>4</sub> (pH < 3) and 0.1 M KH<sub>2</sub>PO<sub>4</sub> + Na<sub>2</sub>HPO<sub>4</sub> (pH 7.0). Water was purified using Millipore Mili-Q purification system in all the experiments.

### 2.2. Electrochemical measurements

Cyclic voltammetry (CV) was performed with a CHI 660 electrochemical workstation (USA) in a conventional three-electrode electrochemical cell using glassy carbon as the working electrode, twisted platinum wire as the auxiliary electrode, and Ag/AgCl as the reference electrode. The glassy carbon electrode (GCE) was polished with 1.0-, 0.3- and 0.05- $\mu\text{m}$   $\alpha\text{-Al}_2\text{O}_3$  powders, successively and sonicated in water for about 5 min after each polishing step. Finally, the GCE was sonicated in water, ethanol, washed with ethanol and dried with high purity nitrogen stream immediately before use.

### 2.3. Modification procedure

The electrochemical modification of a GCE was performed in 0.1 M KCl solution containing 1 mM 4-ABA by potential scanning between 0.5 and 1.4 V (versus Ag/AgCl).

After modification, the electrode was successively rinsed with Milli-Q water and sonicated for 5 min in water to remove the physically adsorbed species. The 4-ABA-modified GCEs were ready for characterization or for further modification [24–27]. Briefly, as shown in Scheme 1, the 4-ABA/GCE was first immersed in an aqueous solution containing 2 mM Cu<sup>2+</sup> (Cl<sup>-</sup>, SO<sub>4</sub><sup>2-</sup>, or NO<sub>3</sub><sup>-</sup>) for 30 min. Then, the electrode was removed, rinsed, and immersed in 2 mM Fe(CN)<sub>6</sub><sup>3-</sup> aqueous solution for 30 min, resulting in a monolayer of CuHCF. Afterwards the modified electrode was removed and rinsed. The electrode modified with CuHCF monolayer immersed alternately in Cu<sup>2+</sup> and Fe(CN)<sub>6</sub><sup>3-</sup> solutions, then the multilayer of CuHCF on 4-ABA/GCE were obtained.

### 2.4. X-ray photoelectron spectroscopy (XPS)

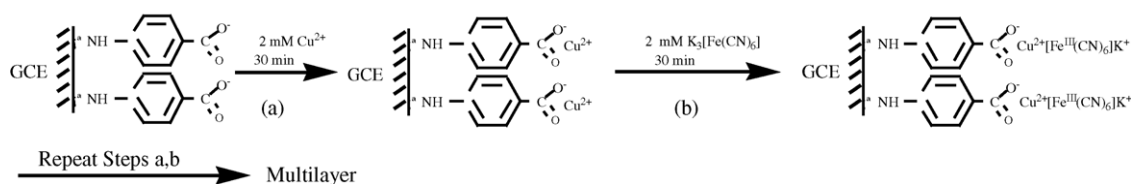
XPS measurement was performed on an ESCALAB-MKII spectrometer (VG Co., U.K.) with an Al K $\alpha$  X-ray radiation as the X-ray source for excitation. The data were obtained at room temperature, and typically the operating pressure in the analysis chamber was below 10<sup>-9</sup> Torr with analyzer pass energy of 50 eV. The resolution of the spectrometer was 0.02 eV.

### 2.5. Electrochemical impedance analysis

Electrochemical impedance measurements were performed with a PARC M398 electrochemical impedance system (EG & Princeton Applied Research, Princeton, NJ) consisting of a potentiostat Model 273 and a computer-controlled PAR Model 5210 lock-in amplifier with EG&G AC impedance software. An ac voltage of 10 mV in amplitude with a frequency range from 0.1 Hz to 60 kHz was superimposed on the dc potential and applied to the studied electrodes. The dc potential was always set up at the formal potential of Fe(CN)<sub>6</sub><sup>3-/4-</sup>. Experimental data of the electrochemical impedance plot were analyzed by applying the nonlinear least squares fitting to the theoretical model represented by a Randles equivalent electrical circuit.

### 2.6. Atomic force microscopy (AFM)

AFM measurements were performed with a Digital Nanoscope IIIa multimode system (DI, Santa Barbara, CA, USA). The images were acquired in the tapping mode. Measurements were made with the Si cantilever in air at



Scheme 1. Schematic of the overall preparative process of CuHCF multilayer on the 4-ABA-modified GCE.

room temperature. The force constant of the cantilever was 0.1–0.6 N/m with the scan rate of 1–2 Hz.

### 3. Results and discussion

#### 3.1. Covalent modification of GCE with 4-ABA in aqueous solution

The oxidation and grafting of 4-ABA on GCE in aqueous solution are similar to that in organic solvent [16]. Fig. 1A shows cyclic voltammograms on GCE at  $10 \text{ mV s}^{-1}$  in a 0.1 M KCl aqueous solution with different concentrations of 4-ABA. We can see that an irreversible oxidation peak appears at  $\sim 0.8 \text{ V}$  in the process of electrochemical oxidation. The current increases with increasing of 4-ABA concentrations in the solution and the peak potential gradually shifts to more positive which may result from one-electron oxidation of the amino group to its corresponding cation radical according to previous works [8–10,30]. Fig. 1B exhibits

cyclic voltammograms of 1 mM 4-ABA in 0.1 M KCl aqueous solution on GCE for different number of cycles, and the peak current of oxidation gradually diminish to background alongside of cycles increasing, because of the 4-ABA monolayer being formed on the surface of GCE that inhibits the successive 4-ABA monolayer from modification. This indicates a film formation coating on the electrode surface.

#### 3.2. X-ray photoelectron spectroscopy of the 4-ABA-Modified GCE

The attachment of amine cation radicals to the carbon electrode surface has been proven by XPS analysis as shown in Fig. 2. At the bare glassy carbon (GC) plate, the characteristic peak of C 1s is similar and occurred at about 284.6 eV for the pure 4-ABA and 4-ABA grafted on GC. There was no characteristic N 1s peak on bare GC plate. N 1s peak was observed at 400.2 eV [31] for pure 4-ABA, resulting from the  $\text{NH}_2$  group of 4-ABA. However, for 4-ABA grafted on GC, the characteristic nitrogen peak of N 1s appeared at 399.4 eV

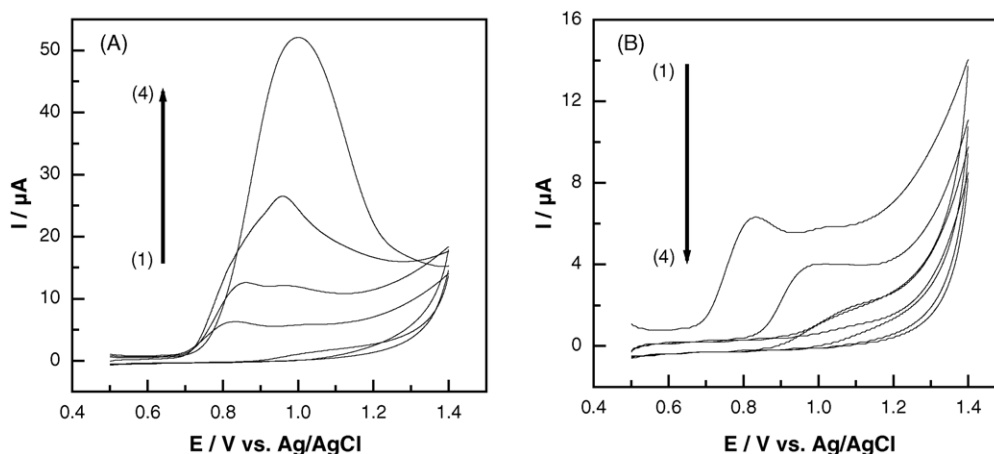


Fig. 1. (A) Cyclic voltammograms on GCE in 0.1 M KCl aqueous solution with different concentrations of 4-ABA: (1) 1, (2) 2.5, (3) 5 and (4) 7 mM; scan rate:  $10 \text{ mV s}^{-1}$ . (B) Cyclic voltammograms on GCE in 0.1 M KCl aqueous solution with 1 mM 4-ABA for the (1) first, (2) second, (3) third and (4) fourth cycles; scan rate:  $10 \text{ mV s}^{-1}$ .

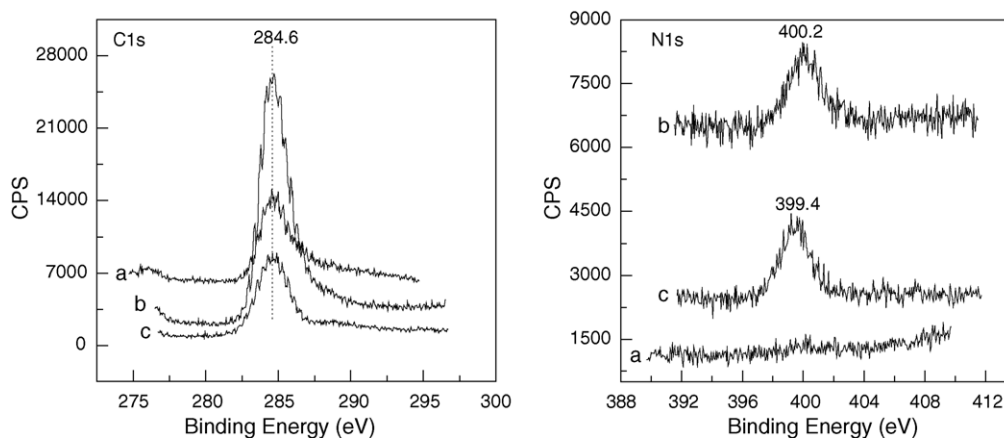


Fig. 2. X-ray photoelectron spectra of C 1s and N 1s for the bare GC plate (a), pure 4-ABA (b) and a GC plate modified with 4-ABA (c).

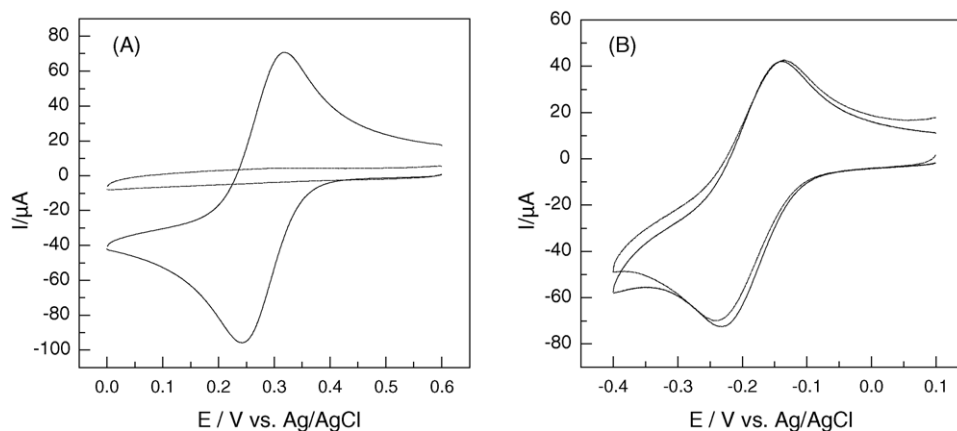


Fig. 3. Cyclic voltammograms on bare (—) and 4-ABA-modified GCE (---) in (A) 5 mM  $\text{Fe}(\text{CN})_6^{3-}$  and (B) 2 mM  $\text{Ru}(\text{NH}_3)_6^{3+}$  PBS solutions (pH 7.0); scan rate:  $100 \text{ mV s}^{-1}$ .

[31] corresponding to the NH group, which indicates that 4-ABA was immobilized on the GC surface. The N 1s peak maximum occurring at 399.9 eV is in accord with the formation of a carbon–nitrogen bond between the amine cation radical and an aromatic moiety of the GC surface [9,10,32].

The 4-ABA monolayer film obtained is very stable in air. Only by mechanically polishing the electrode surface the film can be removed.

### 3.3. Blocking effect of the 4-ABA-modified GCE on electrochemical behavior of $\text{Fe}(\text{CN})_6^{3-}$ and $\text{Ru}(\text{NH}_3)_6^{3+}$ the redox probes

The 4-ABA grafted on GCE surface possesses its terminal carboxyl acid group with a fixed charge depending solution pH. This surface charge states for monolayer-modified electrodes are very significant in both theory and subsequent assembly applications. In high pH buffer solutions ( $\text{pH} \gg \text{pK}_a$ ), carboxyl acid group on the 4-ABA monolayer will dissociate and charge negatively. In contrast, when pH

of the buffer solution is low ( $\text{pH} \ll \text{pK}_a$ ), the carboxyl acid group cannot dissociate and show no net charge. Fig. 3A shows cyclic voltammograms of  $\text{Fe}(\text{CN})_6^{3-}$  on bare GCE (solid line) and the 4-ABA/GCE (dashed line) in PBS buffer solution of pH 7.0. It can be seen that the electron transfer of the  $\text{Fe}(\text{CN})_6^{3-}$  is completely blocked on the 4-ABA/GCE. Fig. 3B shows cyclic voltammograms of  $\text{Ru}(\text{NH}_3)_6^{3+}$  on bare GCE (solid line) and the 4-ABA/GCE (dashed line) in PBS buffer solution of pH 7.0. Obviously, the electron transfer of the  $\text{Ru}(\text{NH}_3)_6^{3+}$  almost does not change on both of the electrodes. Because of carboxyl acid group of the 4-ABA monolayer at pH 7.0 dissociates completely and charges negatively, the negative charged surface will repulse  $\text{Fe}(\text{CN})_6^{3-}$  ions, on the contrary, attract with  $\text{Ru}(\text{NH}_3)_6^{3+}$  ions.

Fig. 4A gives a series of cyclic voltammograms of  $\text{Fe}(\text{CN})_6^{3-}$  in different pH solutions on the 4-ABA monolayer modified electrode. The current response of the  $\text{Fe}(\text{CN})_6^{3-}$  redox probe is related to the pH value of buffer solutions. In low pH ( $\text{pH} < 3$ , curves 1–3) solutions,  $\text{Fe}(\text{CN})_6^{3-}$  exhibits a well-defined redox peak because the

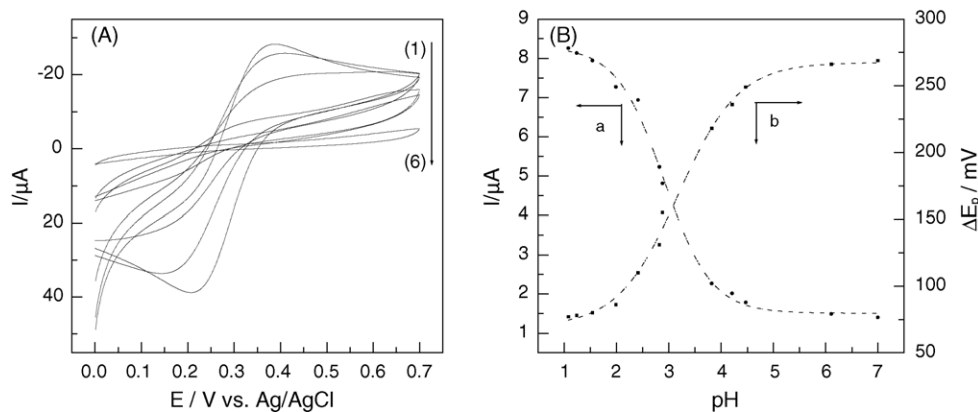


Fig. 4. (A) Cyclic voltammograms of 5 mM  $\text{Fe}(\text{CN})_6^{3-/4-}$  in buffer solutions of pHs at the 4-ABA monolayer modified electrode. Corresponding pH values are (1) 1.99, (2) 2.41, (3) 2.88, (4) 3.82, (5) 4.47 and (6) 5.73, respectively; scan rate:  $10 \text{ mV s}^{-1}$ . (B) Plot of (a)  $I_p$  and (b)  $\Delta E_p$  of the cyclic voltammograms as a function of the solution pH. The cyclic voltammograms were obtained on a 4-ABA/GCE in 1 mM  $\text{Fe}(\text{CN})_6^{3-}$  solutions buffered at different pHs.

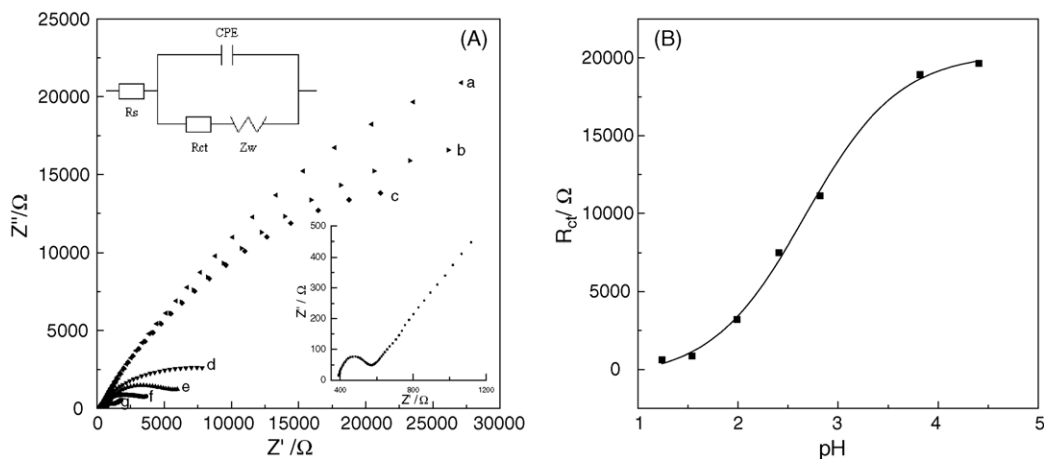


Fig. 5. (A) Impedance plots on a 4-ABA-modified GCE in 5 mM  $\text{Fe}(\text{CN})_6^{3-/4-}$  solutions of different pHs: (a) 7.0, (b) 6.11, (c) 5.73, (d) 4.47, (e) 3.82, (f) 2.82, (g) 2.41. The top inset shows the equivalent circuit model for the analysis of the impedance data. The bottom inset shows the impedance plot of a bare GCE in 5 mM  $\text{Fe}(\text{CN})_6^{3-/4-}$  PBS (pH 7.0). (B) Plot of charge-transfer resistance  $R_{ct}$  as a function of solution pH.

carboxyl acid groups on the 4-ABA monolayer modified electrode is not dissociated, so the electrode surface is uncharged and  $\text{Fe}(\text{CN})_6^{3-}$  can easily exchange electron with GCE surface. On the contrary, when pH value of the buffer solution is over 3 (curves 4–6), the electron transfer of  $\text{Fe}(\text{CN})_6^{3-}$  with GCE surface is gradually blocked. Resulting from that electrostatic repulsion exists between the redox probe and the modified electrode surface. Based on the fundamentals calculated the surface  $\text{p}K_a$  on modified electrode using voltammetry [33], the surface  $\text{p}K_a$  of the 4-ABA monolayer film is estimated to be about 3.0 from  $I_p$ -pH curve (a) in Fig. 4B. A similar  $\text{p}K_a$  (3.1) is also obtained from the  $\Delta E_p$ -pH curve (b) in Fig. 4B. These results are smaller than those for 4-aminobenzoic acid in solution ( $\text{p}K_a = 4.6$ ) [34].

#### 3.4. Electrochemical impedance spectroscopy (EIS) measurement of $\text{Fe}(\text{CN})_6^{3-/4-}$ on 4-ABA-modified GCE under different pH conditions

Fig. 5 shows the ac impedance spectroscopic results of 5 mM  $\text{Fe}(\text{CN})_6^{3-}/\text{Fe}(\text{CN})_6^{4-}$  on the 4-ABA monolayer GC electrode in different pH solutions. The profiles exhibit a semicircle part followed by a linear part (in Fig. 5A). The semicircle part at high frequencies corresponds to the electron transfer limited process; and the linear part at low frequencies corresponds to the diffusion process. To give more detailed information about the electrode/solution interfaces, the Randles circuit (inset Fig. 5A) is chosen to fit the obtained impedance data [35]. CPE expresses a constant phase element, which is used instead of a pure capacitor in the equivalent circuit due to microscopic surface roughness and inhomogeneity,  $R_{ct}$ , the charge-transfer resistance,  $Z_w$ , Warburg impedance, and  $R_s$ , the solution resistance. The impedance data were analyzed using this electrical equivalent circuit. Thus, the electron transfer resistance,  $R_{ct}$ , could be estimated, which equals to 313  $\Omega$  for the bare GC elec-

trode in pH 7.0 solution. The value of  $R_{ct}$  about the modified varied with pH as shown in Fig. 5B. Compared with the bare GC electrode, the electrode showed a larger  $R_{ct}$  after modified with 4-ABA. The results indicate that 4-ABA plays an important role similar to a non-conductive layer and makes the electron transfer more difficulty. The  $R_{ct}$  of the modified electrode increases dramatically with the increase of pH, due to the inhibition of the electron transfer. It is possible that the full deprotonation of carboxyl groups causes some surface structure change on the 4-ABA film as pH increasing, which completely blocks the electrode surface, although the reason for this blocking is not very clear. According as the fundamentals calculated the surface  $\text{p}K_a$  using electrochemical impedance spectroscopy (EIS) [36], the value of  $\text{p}K_a$  could be estimated to be 2.8 from the  $R_{ct}$ -pH plot, which is close to those values obtained from the  $I_p$ -pH and  $\Delta E_p$ -pH plots (in Fig. 5B).

As described above,  $R_{ct}$  increase with pH in the solution is due to the inhibition for the electron transfer of the redox probe [37]. The increase in the charge-transfer resistance is related to the electrode coverage and is given by [35]

$$(1 - \theta) = \frac{R_{ct}^0}{R_{ct}} \quad (1)$$

where  $\theta$  is the apparent electrode coverage, assuming that all the currents are passed via bare spots on the electrode, and  $R_{ct}^0$  and  $R_{ct}$  represent the charge-transfer resistance measured on a bare and a modified GC electrode, respectively. Compared with the bare GC electrode, the electrode has a larger  $R_{ct}$  after modified with 4-ABA which equals to 104325  $\Omega$ . Using Eq. (1), the surface coverage was calculated to be 99.7%.

#### 3.5. Fabrication of CuHCF multilayer films on 4-ABA-modified GCE

Layer-by-layer assembly based on complexation was used to build up multilayer films. Following the attachment of

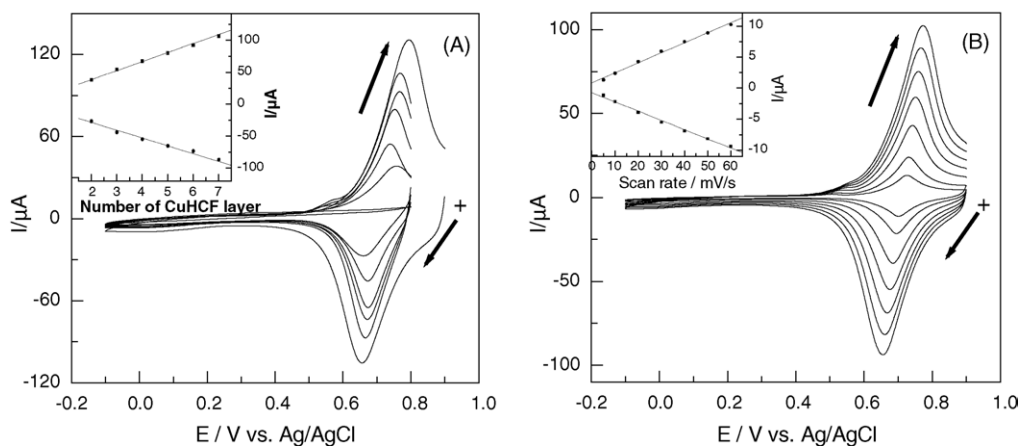
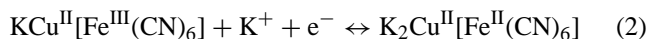


Fig. 6. (A) Cyclic voltammograms of one to seven CuHCF layers in 0.1 M KCl solution; scan rate: 50 mV s<sup>-1</sup>. (B) Cyclic voltammograms of seven layers of CuHCF in 0.1 M KCl solution with different scan rates: 5, 10, 20, 30, 40, 50 and 60 mV s<sup>-1</sup>.

4-ABA to the GCE in 0.1 M KCl aqueous solution, the derivative electrode surface with COOH group was alternately placed in Cu<sup>2+</sup> and Fe(CN)<sub>6</sub><sup>3-</sup> solutions for 30 min (assembly process shows in Scheme 1). After each modification, cyclic voltammetry was used to characterize the increase in quantity of modifiers loaded on the multilayer films. Fig. 6A shows the cyclic voltammograms of the as-prepared multilayer films (CuHCF as the outermost layers) with different number of CuHCF layers in 0.1 M KCl aqueous solution. An unobvious redox peak appearing at 0.55 V is assigned to the Cu<sup>2+/+</sup> redox couple. Another pair of redox peaks with a formal potential of about 0.8 V is assigned to the low-spin Fe<sup>II/III</sup> redox couple [21] in the CuHCF. The redox reaction can be written as follows:



As shown in Fig. 6A, the growth of CuHCF multilayer films is demonstrated by linearly increasing of peak current with the layer number except that the peak current of the first layer is not obvious. In Fig. 6B shows cyclic voltammograms of the seven layers CuHCF at different scan rates in the potential

range of -0.1 to 0.9 V in 0.1 M KCl aqueous solution. The peak current of CuHCF is increased linearly with increasing of scan rate, this indicates that the electrochemical behavior of CuHCF deposited in the multilayer films corresponds to a surfaced-confined and reversible electron transfer process at lower scan rates. From XPS of Fig. 7 the existence of Cu, Fe in the multilayer can be seen clearly. The characteristic peaks of Cu2p and Fe2p occur at about 935.3 and 708.5 eV, respectively. Cu and Fe are bivalent in comparison with standard data. This result is inconsistent with Eq. (2).

The surface morphology of the multilayer films was examined by atomic force microscopy. Shown in Fig. 8 tapping-mode AFM images of CuHCF multilayer films on 2 Cu<sup>2+</sup>/2 Fe(CN)<sub>6</sub><sup>3-</sup> (B) and 7 Cu<sup>2+</sup>/6 Fe(CN)<sub>6</sub><sup>3-</sup> (C), respectively, and on 4-ABA/GCE (A). The thickness of multilayer nanoconstruction increases and the accumulation of nanoparticles is more and more compact with increasing layer numbers. The surface roughness of the 7 Cu<sup>2+</sup>/6 Fe(CN)<sub>6</sub><sup>3-</sup> multilayer changes to 11.28 nm from 8.91 nm of the 2 Cu<sup>2+</sup>/2 Fe(CN)<sub>6</sub><sup>3-</sup>. And the surface roughness of the 4-ABA/GCE is 3.54 nm.

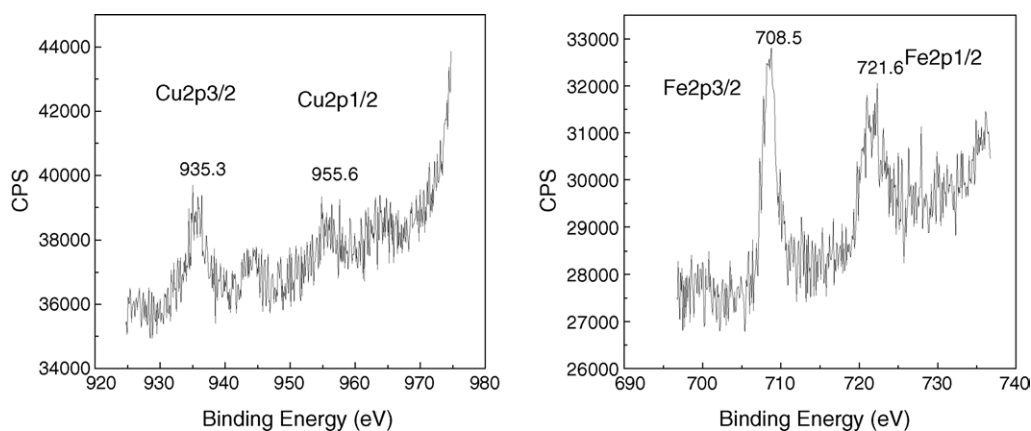


Fig. 7. X-ray photoelectron spectra of Cu 2p, Fe 2p energy levels for seven CuHCF multilayers.

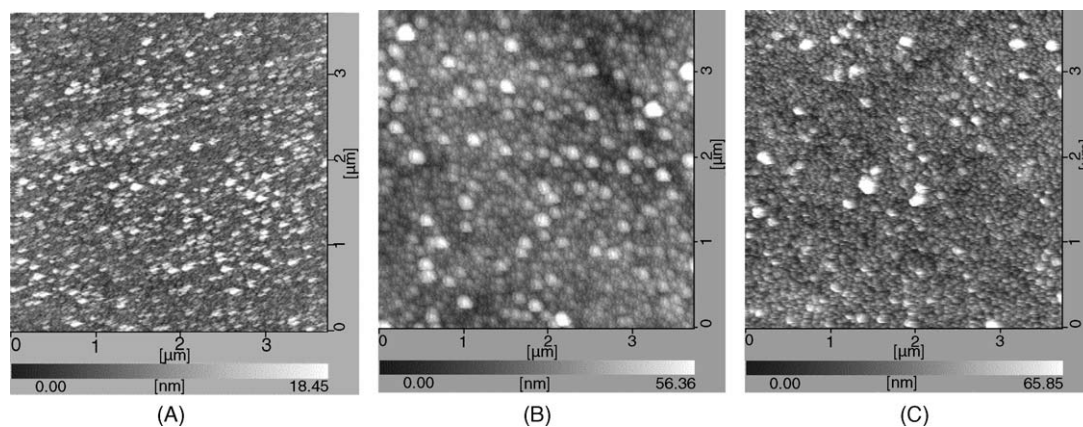


Fig. 8. AFM image of the GC plate modified with 4-ABA (A), two CuHCF multilayer films with  $\text{Fe}(\text{CN})_6^{3-}$  as the outermost layer (B) and seven CuHCF multilayer films with  $\text{Cu}^{2+}$  as the outermost layer (C).

#### 4. Conclusion

In this paper, we have accomplished the chemically modification on GCE via the electrochemical oxidation of 4-ABA in aqueous solution and it has been proved by X-ray photoelectron spectroscopy, cyclic voltammetry and electrochemical impedance. The 4-ABA monolayer films on GCE prepared in aqueous solution have good stability. The dissociable terminal carboxyl groups on the 4-ABA/GCE have a major effect on blocking of the anionic redox probe  $\text{Fe}(\text{CN})_6^{3-}$  which can be controlled by changing the solution pH. Cyclic voltammetry and electrochemical impedance experiments have been reliably used as convenient and precise methods to estimate the surface  $\text{p}K_a$  of the 4-ABA film grafted on GCE. The 4-ABA-modified GCE has been used as a precursor substrate for construction of CuHCF multilayer film by layer-by-layer assembling. This multilayer film has good stability, uniformity and distinct electrochemical behavior.

#### Acknowledgment

The authors thank the National Science Foundation of China (no. 20275036, no. 20211130506).

#### References

- [1] M. Fujihira, A. Tamana, T. Osa, *Chem. Lett.* 64 (1977) 361.
- [2] Y.-C. Liu, R.L. McCreery, *Anal. Chem.* 69 (1997) 2091.
- [3] J.F. Evans, T. Kuwana, *Anal. Chem.* 51 (1979) 358.
- [4] C.M. Elliott, C.A. Marrese, *J. Electroanal. Chem.* 119 (1981) 395.
- [5] P. Allongue, M. Delamar, B. Desbat, O. Fagebarme, R. Hitmi, J. Pinson, J.-M. Savéant, *J. Am. Chem. Soc.* 119 (1997) 201.
- [6] M. Delamar, R. Hitmi, J. Pinson, J.-M. Savéant, *J. Am. Chem. Soc.* 114 (1992) 5883.
- [7] C. Bourdillon, M. Delamar, C. Demaille, R. Hitmi, J. Moiroux, J. Pinson, *J. Electroanal. Chem.* 336 (1992) 113.
- [8] B. Barbier, J. Pinson, G. Desarmot, M. Sanchez, *J. Electrochem. Soc.* 137 (1990) 1757.
- [9] R.S. Deinhammer, M. Ho, J.W. Anderegg, M.D. Porter, *Langmuir* 10 (1994) 1306.
- [10] A.J. Downard, A. Mohamed, *Electroanalysis* 11 (1999) 418.
- [11] H. Tanaka, A. Aramata, *J. Electroanal. Chem.* 437 (1997) 29.
- [12] K. Takehara, H. Takemura, Y. Ide, *Electrochim. Acta* 39 (1994) 817.
- [13] T.A. Jones, G.P. Perez, B.J. Johnson, R.M. Crooks, *Langmuir* 11 (1995) 1318.
- [14] J. Liu, S. Dong, *Electrochem. Commun.* 2 (2000) 707.
- [15] J. Liu, L. Cheng, B. Liu, S. Dong, *Electroanalysis* 13 (2001) 993.
- [16] J. Liu, L. Cheng, B. Liu, S. Dong, *Langmuir* 16 (2000) 7471.
- [17] B. Ortiz, C. Saby, G.Y. Champagne, D. Bélanger, *J. Electrochem. Chem.* 455 (1998) 75.
- [18] Y.-C. Liu, R.L. McCreery, *Anal. Chem.* 69 (1997) 4680.
- [19] X. Li, Y. Wan, C. Sun, *J. Electroanal. Chem.* 569 (2004) 79.
- [20] K. Morita, A. Yamaguchi, N. Teramae, *J. Electroanal. Chem.* 563 (2004) 249.
- [21] S. Bharathi, M. Nogami, S. Ikeda, *Langmuir* 17 (2001) 7468.
- [22] P.M.S. Monk, R.J. Mortimer, D.R. Rosseinsky, *Electrochromism, Fundamentals and Applications*, VCH, Weinheim, 1995 (Chapter 6).
- [23] K. Itaya, I. Uchida, V.D. Neff, *Acc. Chem. Res.* 19 (1986) 162.
- [24] O. Kahn, *Nature* 378 (1995) 667.
- [25] O. Sato, T. Iyoda, A. Fujishima, K. Hashimoto, *Science* 272 (1996) 704.
- [26] C. Lin, A.B. Bocarsly, *J. Electroanal. Chem.* 300 (1991) 325.
- [27] D. Zhou, H.-X. Ju, H.-Y. Chen, *J. Electroanal. Chem.* 408 (1996) 219.
- [28] W. Cheng, S. Dong, E. Wang, *Chem. Mater.* 15 (2003) 2495.
- [29] S. Bharathi, V. Yegnaraman, R.G. Prabhakara, *Langmuir* 11 (1995) 6663.
- [30] M. Masui, H. Sayno, Y. Tsuda, *J. Chem. Soc. B* (1968) 973.
- [31] D.J. Bartkowiaka, B.N. Kolarza, W. Tylus, *Polymer* 44 (2003) 5797.
- [32] R. Nordberg, R.G. Albridge, T. Bergmark, U. Ericson, J. Hedman, C. Nordling, B.J. Siegbahn, *Ark. Kemi.* 28 (1968) 257.
- [33] J. Zhao, L. Luo, X. Yang, E. Wang, S. Dong, *Electroanalysis* 11 (1999) 1108.
- [34] H.C. Brill, *J. Am. Chem. Soc.* 43 (1921) 1320.
- [35] A.J. Bard, L.R. Faulkner, *Electrochemical Methods*, John Wiley & Sons, New York, 1980, p. 316.
- [36] V. Molinero, E.J. Calvo, *J. Electroanal. Chem.* 455 (1998) 17.
- [37] F. Patolsky, M. Zayats, E. Katz, I. Willner, *Anal. Chem.* 71 (1999) 3171.